

Conformational Assignment, Absolute Configuration, and Chiral Separation of All the Stereoisomers Created by the Combined Presence of Stereogenic Centers and Stereogenic Conformational Axes in a Highly Hindered 1,5-Naphthyl Sulfoxide

Daniele Casarini and Lodovico Lunazzi*

Dipartimento di Chimica Organica "A. Mangini", Università, Via Risorgimento 4, Bologna, 40136 Italy

Francesco Gasparrini* and Claudio Villani

Dipartimento di Studi di Chimica e Tecnologia delle Sostanze Biologicamente Attive, Università "La Sapienza", P. le A. Moro 5, Roma, 00185 Italy

Maurizio Cirilli and Enrico Gavuzzo

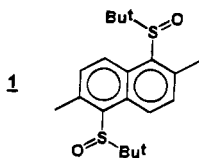
Istituto di Strutturistica Chimica, CNR, Via Salaria, Monterotondo, 00016 Italy

Received October 4, 1994*

The presence of two stereogenic centers and of two stereogenic conformational axes in 2,6-dimethyl-1,5-bis(2-methyl-2-propylsulfinyl)naphthalene (**1**) entails the existence of 10 stereoisomers. In particular, both the meso form (**1a**) and the racemic form (**1b**) are constituted by three atropisomers; in the case of the latter (**1b**) each of them entails a pair of enantiomers (total of six species), whereas owing to the symmetry only one of the three atropisomers of the meso form (**1a**) yields a pair of enantiomers (a total of four species). Despite the low conformational interconversion barrier (18.5 kcal/mol) all of them have been separated by low temperature (-45 °C) chiral HPLC. Their configurational and conformational assignment has been achieved by a combined use of NMR (both in solution and solid state) and on-line CD-detected chiral HPLC. The single crystal X-ray diffraction yielded the absolute configuration of one of the stereoisomers ((*ZR,ER*)-**1b**) from which all the others could be obtained by CD relationship.

Introduction

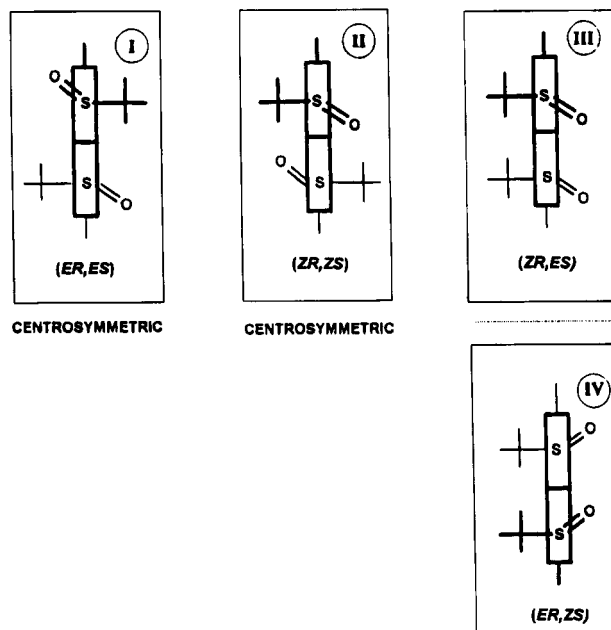
It has been shown that hindered 1-naphthyl sulfoxides (ArSOR, where Ar = 2-methylnaphthyl) entail a pair of conformational diastereoisomers (atropisomers) owing to the simultaneous presence of a stereogenic center (the sulfur atom) and of a conformational stereogenic axis (C1-SO). In the case of R = *tert*-butyl the two atropisomers could be detected by NMR even at room temperature, as the rotation about the C1-SO axis is sufficiently slow on the NMR time scale. The multiplication of such stereogenic centers and axes is bound to create a much more complex situation. When 2,6-dimethylnaphthalene, for instance, is substituted at position 1,5 by two *t*-BuSO moieties (**1**), the two stereogenic centers (sulfur atoms) would yield two configurationally stable diastereoisomers: (*RS*) meso, **1a**, and (*RR* and *SS*) racemic, **1b**. Each



of them, in addition, can generate a number of stereolabile atropisomers, owing to the restricted rotation about the two conformational stereogenic axes (i.e., C1-SO and C5-SO).

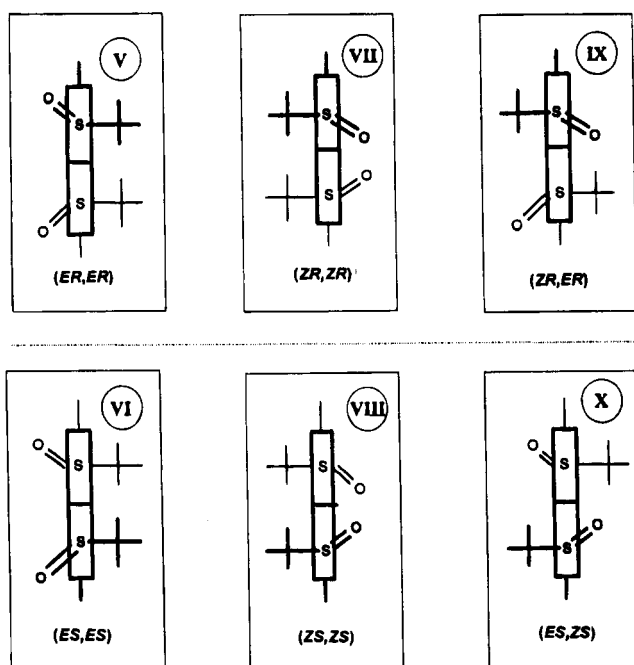
In Chart 1 it is shown how three such atropisomers (*EE*, *ZZ*, and *ZE*) are expected to occur in the case of the meso compound (**1a**). Furthermore, the atropisomer *ZE* entails a pair of enantiomers (*ZR,ES* and *ZS,ER*) as its

Chart 1. **1a**, (*R,S*) Meso



two mirror images (III and IV of Chart 1) are not superimposable as long as the rotation rates about the two Ar-SO axes are slow. Three atropisomers are equally expected for the racemic diastereoisomer **1b**, each of them being constituted by a pair of enantiomers, since the sulfur atoms can have either the *RR* or the *SS* configuration (Chart 2). As many as 10 stereoisomers are thus predicted for **1** (i.e., I-IV of Chart 1 and V-X of Chart 2). The separation and the identification of all such species is the purpose of the present work.

* Abstract published in *Advance ACS Abstracts*, November 15, 1994.

Chart 2. **1b**, (*R,R*) and (*S,S*) Racemic

Results and Discussion

Oxidation of 2,6-dimethyl-1,5-bis(2-methyl-2-propylthio)naphthalene with 3-chloroperbenzoic acid at $-30\text{ }^{\circ}\text{C}$ yields the disulfoxide **1** as a chromatographically separable (silica gel) mixture of **1a** and **1b**. The less abundant isomer (ca. 30%) was identified as **1b** (racemic) as it could be separated into a pair of enantiomers by HPLC on a chiral stationary phase (CSP) [(*R,R*)-DACH-DNB stationary phase];¹ on the contrary, the major isomer gave a single peak on the same chiral column and was consequently identified as **1a** (meso).

The 600 MHz ^1H NMR spectrum of the *tert*-butyl region of the latter clearly shows (in toluene- d_6) the presence of the three expected atropisomers (Figure 1, top). The two single lines at 1.053 and 1.048 ppm correspond, respectively, to the most (77%) and to the least (5%) abundant atropisomers to which, consequently, the achiral conformations *EE* or *ZZ* (I and II of Chart 1) must be assigned. The pair of equally intense lines (9% each) at 0.998 and 1.012 ppm must be attributed to the racemic *ZE* atropisomer (population 18%) which is expected to display two *tert*-butyl signals, one being *syn* and the other *anti* to the oxygen of the neighboring SO group (III and IV of Chart 1).

Whereas the lines of the *tert*-butyl groups are not appropriate to assign the *ZZ* or the *EE* conformation of the two achiral atropisomers a reliable assignment can be achieved by using the lines of the corresponding 2-methyl groups. As shown in Figure 1 (top) these signals are widely separated in that those in a position *syn* to the SO moiety are shifted downfield^{2,3} with respect to those in position *anti*. Thus, the most abundant atropisomer (77%) corresponds the *ZZ* conformer since its 2-Me signal is at higher field (2.177 ppm). For the same reason to the least abundant (5%) atropisomer the *EE* conformation must be assigned, since its 2-Me signal

is at lower field (2.931 ppm). The chiral *ZE* atropisomer (18%) should display a pair of 2-Me signals: that *syn* to SO is observed at lower (2.918 ppm) and that *anti* to SO at higher field (2.182 ppm), very close to the intense signal of the *ZZ* atropisomer.

A convincing confirmation of this attribution comes from a lanthanide induced shift (LIS) experiment.⁴ Upon addition of increasing amounts of $\text{Eu}(\text{fod})_3$ to a CDCl_3 solution of **1a**, the 2-Me signal of the less abundant (5%) atropisomer experiences the largest downfield displacement (the slope of the straight line relating the shifts to the $\text{Eu}(\text{fod})_3/\mathbf{1a}$ molar ratio being 4.3 ppm). The downfield line (2.918 ppm) of the chiral atropisomer (18%) also exhibits a substantial displacement (3.0 ppm), whereas the line of the most abundant (77%) atropisomer is hardly affected (0.35 ppm). Since the proton NMR signals of the 2-Me groups *syn* to the SO moiety are known^{2,4} to have a large LIS effect and those that are *anti* are much less affected, these values indicate that the 5% atropisomer must have the *EE* conformation (both methyl groups are *syn* to the SO moiety), the 18% atropisomer the *EZ* conformation (only one methyl group is *syn* to SO moiety), and the 77% atropisomer the *ZZ* conformation (both methyl groups are *anti* to the SO moiety).

The solid state ^{13}C CP-MAS spectrum of **1a** (75.5 MHz) displays three different *t*-Bu signals with 1:1:1 intensity ratio (23.7, 25.8, and 26.4 ppm) for the three methyls of the *tert*-butyl group, to be compared with the single line (25.5 ppm) observed in CDCl_3 for the major conformer of **1a**. This is the consequence of a restricted rotation about the *t*-Bu-SO bond in the solid state.⁵ Contrary to the solution spectra, the solid state spectrum of **1a** does show that a single atropisomer is present in the crystalline state. An analogous feature has been observed for the racemic diastereoisomer **1b**, which also displays a solid state spectrum appropriate for a single atropisomer with nonequivalent signals for the methyl groups of the *tert*-butyl moiety. In **1b** only two *t*-Bu lines, having however a 2:1 relative intensity (24.5 and 22.6 ppm respectively), are observed. The existence of only one of the possible conformers in the solid state is a feature usually observed in flexible molecules like the present ones.

On warming the toluene solution of **1a** above room temperature the spectral lines corresponding to the various atropisomers broaden and eventually coalesce in a reversible manner, owing to the increasing rotation rate about the Ar-SO bonds. A line shape analysis of the 2-Me signals (at 200 MHz) gave the rate constants at different temperatures, hence the ΔG^\ddagger values (18.5 kcal/mol) for the interconversion process. Since at 200 MHz the two downfield lines almost overlap as do the two upfield lines, the system had to be treated as an exchange between two unequally populated sites. As it appears unconceivable to consider a simultaneous rotation of both the RSO groups, the interconversion between the two achiral (*ZZ* and *EE*) atropisomers necessarily requires the passage through the chiral *ZE* atropisomer. As a

(4) $\text{Eu}(\text{fod})_3$ stands for europium 1,1,1,2,2,3,3-heptafluoro-7,7-dimethyl-4,6-octane dithionate. See: Cockerill, H. F.; Davies, G. L. O.; Harden, R. C.; Rackham, D. M. *Chem. Rev.* **1973**, *73*, 533.

(5) The low-temperature ^1H (200 MHz) spectrum of **1a** in CH_2Cl_2 displays a broadening of the *tert*-butyl line of the major conformer, extremely more pronounced than that of the corresponding 2-Me line. At $-135\text{ }^{\circ}\text{C}$ the former signal becomes so broad as to suggest the coalescence of signals undergoing an exchange process. This confirms the existence of a restricted rotation about the *t*-Bu-SO bond which would make the three methyl groups anisochronous. Unfortunately, direct detection of these three signals in solution is prevented by the precipitation of **1a** below $-135\text{ }^{\circ}\text{C}$.

(1) Gasparrini, F.; Misiti, D.; Villani, C. *Chirality* **1992**, *4*, 447.

(2) Casarini, D.; Foresti, E.; Gasparrini, F.; Lunazzi, L.; Macciantelli, D.; Misiti, D.; Villani, C. *J. Org. Chem.* **1993**, *58*, 5674.

(3) (a) Fraser, R.; Schuber, F. J. *Can. J. Chem.* **1970**, *48*, 633. (b) Lett, R.; Marquet, A. *Tetrahedron* **1974**, *30*, 3379.

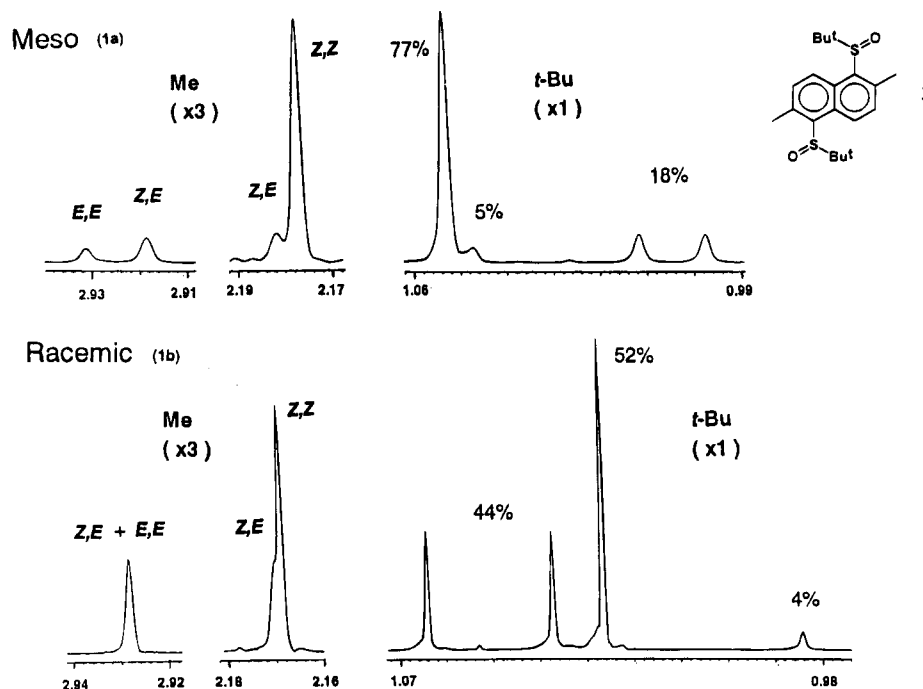


Figure 1. Aliphatic region of the ^1H NMR spectra (600 MHz) of **1a** (top) and **1b** (bottom) in $\text{toluene-}d_8$. Right: *tert*-butyl signals with the indication of the relative proportion of the three atropisomers. Left: signals of the methyl groups in positions 2,6 (for convenience vertically amplified by a factor of 3) with the indication of the proposed assignment.

consequence two transition states should be, in principle, considered. The experimental accuracy of the line shape analysis, however, did not allow a distinction between the two barriers: the value of 18.5 kcal/mol thus represents the energy difference between the most stable (*ZZ*) ground state and the highest of the two possible transition states. The latter, however, are expected to have very similar energies as the rotation of one of the two RSO groups should not be sensibly affected by the conformation (*E* or *Z*) adopted by the second RSO group, which lies quite farther away.

The results of molecular mechanics calculations⁶ suggest indeed that the energy of the transition state for the interconversion of *ZZ* into *ZE* is only 0.7 kcal/mol lower than that for the interconversion of *ZE* into *EE*. The same calculations also indicate that the rotation involving the passage of the *tert*-butyl group over C-8 is preferred with respect to the passage over the methyl group in position 2, the corresponding computed barrier being 3 kcal/mol lower. The barrier calculated with the latter model (19.7 kcal/mol) is in reasonable agreement with the measured value (18.5 kcal/mol). Also, the trend of the computed ground state energies (*ZZ* more stable than *ZE* and *EE* by 0.8 and 1.4 kcal/mol respectively) agrees well with the experimental assignment.

The 600 MHz proton NMR spectrum of the racemic diastereoisomer **1b** in $\text{toluene-}d_8$ also shows the presence of three atropisomers (Figure 1, bottom). Inspection of the *tert*-butyl signals shows that the proportion of the *ZE* atropisomer (which according to Chart 2 must exhibit

a pair of equally intense lines) is only slightly lower (44%) than that of the most stable atropisomer (52%), the third being about 4%. In more polar solvents (CDCl_3 or $\text{CD}_2\text{-Cl}_2$) *ZE* becomes the most stable (50%) species, the other two being 46% and 4%. The shifts (in $\text{toluene-}d_8$) of the 2-Me groups of **1b** allow us to assign the *ZZ* conformation to the atropisomer with a 52% proportion as its single signal is at high field (2.169 ppm), very close to one of the two lines (the one corresponding to the 2-methyl group *anti* to SO) of the *ZE* atropisomer (2.170 ppm). The minor (4%) atropisomer must have the *EE* conformation, as indicated by the low field shift (2.928 ppm) of its line which overlaps with the second line of the *ZE* atropisomer (i.e., the one corresponding to the 2-Me group *syn* to SO).

Separation of the stereoisomers of **1** has been accomplished by HPLC on a "brush-type" chiral stationary phase (CSP) containing the bis(3,5-dinitrobenzoyl) derivative of (*R,R*)-1,2-diaminocyclohexane¹ as chiral selector. Under conditions of fast (with respect to the chromatographic time scale) rotation around the $\text{C}_{\text{Ar}}\text{-SO}$ axis, compound **1** is expected to give three peaks on the CSP, corresponding to the meso form (**1a**) and to the pair of enantiomers of **1b**. The experimental parameters that can be varied to reach the fast exchange situation, where the contribution of the dynamic process to band broadening is negligible, are the column temperature, its length and the eluent flow rate. By using a standard column and typical HPLC flow rate (250×4 mm and 2.0 mL/min, respectively), three well-separated sharp peaks are observed at 65 °C (pertinent chromatographic data are given in Table 1). The first eluting peak, whose relative area is about 70%, corresponds to the meso form **1a**, as it does not display any signal when on-line monitored by CD in the wavelength region between 310 and 320 nm.⁷ On the contrary, the second and third eluted peaks, of equal intensity, show two CD signals of opposite sign at 320 nm and, therefore, correspond to the (*R,R*) and

(6) We made use of the MMX force field as implemented in the program PC Model, Serena Software, Bloomington, IN. See also: Gajewski, J. J.; Gilbert, K. K.; McKelvey, J. *Advances in Molecular Modelling*, JAI Press: Greenwich, 1992; Vol. 2. As no particular parameters were available for sulfoxides those of default were employed. The barriers were computed by driving Ar-SO torsion angle in 2° steps in the proximity of 0° and 180° and allowing the other angles and bond distances to relax to their minima for each of the fixed values of the torsion angle.

Table 1. Chromatographic Data at 65 °C for the Resolution of Sulfoxides **1a and **1b** on (*R,R*)-CSP (250 × 4 mm). *n*-Hexane/2-Propanol/Methanol (70:30:10) Used as Eluent with a 2.0 mL/min Flow Rate**

compd	k' ^a	α^b
1a (<i>R,S</i>)	3.35	
1b (<i>R,R</i>)	4.53	1.27
1b (<i>S,S</i>)	5.75	

^a The capacity factor is defined as $(t_1 - t_0)/t_0$ where t_1 is the retention time and t_0 is the hold-up time. ^b The enantioselectivity factor is defined as the ratio of the capacity factors of the second and first eluted enantiomers.

(*S,S*) enantiomers of **1b**, respectively. The elution order could be unambiguously determined by a single crystal X-ray analysis carried out on the first eluted enantiomer (see further) and conforms with the elution order of the parent monosulfinyl compound² on the same CSP. Upon switching to the "racemic version" of the same CSP (i.e., achiral HPLC on a sorbent containing the same functional groups of the CSP, but with *ee* = 0), signal averaging is observed for the two last eluting peaks, thus confirming the assignments based on UV/CD on-line detections.

The value of the NMR measured conformational interconversion barrier for **1a** indicates that at temperatures lower than -30 °C the lifetimes of the atropisomers should be long enough (about 30 min) to allow their physical separation. However, because of the large number of peaks expected for **1** at low temperatures, **1a** and **1b** were separated by preparative HPLC on silica gel and then separately analyzed on the chiral column. Even in this simplified situation, the low barrier of the exchange processes between four exchanging species in the case of **1a** and between three exchanging species of two equally populated sets in the case of **1b** makes the atropisomers HPLC separation a nontrivial one.

In order to avoid peak distortions caused by on-column isomerization phenomena, the total analysis time should be much smaller than the half-life time of the exchanging species at a given temperature: for this reason, a shorter chiral column (100 × 4 mm) and a more polar eluent (CH₂Cl₂/CH₃OH, 60:1) were used in the variable temperature chromatography of **1a** and **1b** (see Table 2).

The dynamic pattern obtained in the case of **1a** is shown in Figure 2 where a single, broad peak is observed at 25 °C which, with decreasing temperature, becomes progressively sharper. At the same time additional peaks emerge from the interconversion zone, situated at the rear of the principal peak, and at -45 °C the four expected peaks are eventually detected. In agreement with the NMR results, the most and the least intense peaks correspond, respectively, to the achiral atropisomers *ZZ* (80%) and *EE* (2%) as they give no signal when CD monitored at 310 nm. The two most retained peaks (global intensity 18%) correspond to the couple of enantiomers *ZR,ES* and *ZS,ER* predicted for the *ZE* atropisomer, as they show two oppositely signed CD signals. Accordingly, when using the racemic version of the CSP at -45 °C, only three peaks, rather than four, are detected, the most retained two having merged into a single one.

The NMR spectrum of racemic **1b** obviously could not discriminate between the pairs of configurational enan-

Table 2. Chromatographic Data for the Resolution of Sulfoxides **1a and **1b** on (*R,R*)-CSP (100 × 4 mm). CH₂Cl₂/Methanol (60:1) Used as Eluent with a 2.0 mL/min Flow Rate at a Temperature of -45 °C**

compd	k' ^a	α^b
1a (meso)		
<i>ZR,ZS</i>	3.00	
<i>ER,ES</i>	4.13	
<i>ZR,ES</i> ^c	11.38	1.03
<i>ER,ZS</i> ^c	11.79	
1b (racemic)		
<i>ZR,ER</i>	1.38	3.01
<i>ZS,ES</i>	4.15	
<i>ER,ER</i>	2.69	2.77
<i>ES,ES</i>	7.46	
<i>ZR,ZR</i>	7.46	1.42
<i>ZS,ZS</i>	10.62	

^{a,b} See Table 1 for explanations. ^c The elution order of the chiral atropisomers of **1a** has not been established.

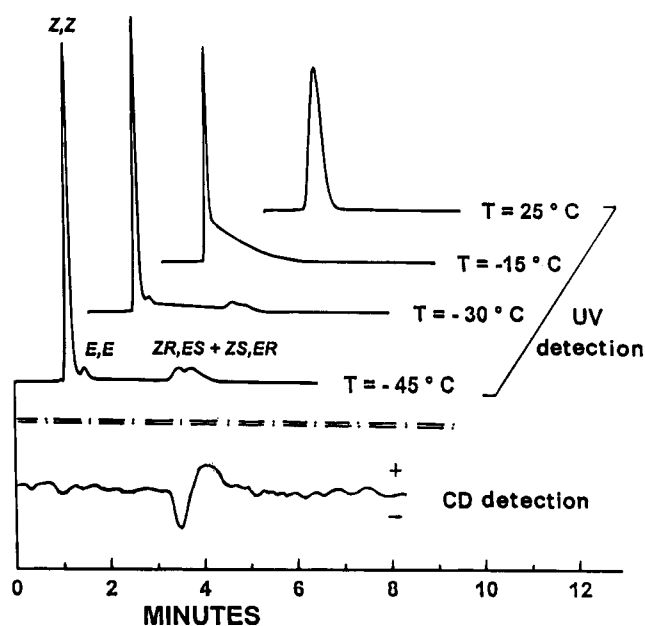


Figure 2. UV (310 nm) and CD (310 nm) detected dynamic HPLC of **1a** on the (*R,R*)-CSP (see Table 2 for other details).

tiomers (due to the stereogenic sulfur atoms) predicted for each of the three atropisomers, but they could be identified by chiral HPLC at low temperature. The variable temperature chromatography of **1b**, carried out under the same experimental conditions used for **1a**, is shown in Figure 3. At 25 °C two poorly resolved, broad peaks are observed for the *R,R* and *S,S* enantiomers. On lowering the temperature they broaden further (at 0 °C) and then split into four peaks connected by an intermediate isomerization region at -15 °C and decoalesce completely at -45 °C. Actually, five peaks rather than six are observed at this temperature, because one conformer of the *R,R* enantiomer has the same capacity factor of a different conformer of the *S,S* enantiomer (see below). On the racemic version of the CSP, three peaks of relative intensity 52:5:43 are observed at -45 °C, corresponding to the three possible atropisomers of **1b**. The intensity distribution⁸ parallels that observed in the NMR spectrum of **1b** in the same solvent (CD₂Cl₂); thus, the least retained atropisomer (52%) must have the *Z,E* conformation, and the *E,E* conformation has to be assigned to the least abundant atropisomer (5%).

(7) The on-line recorded UV spectrum of the first eluting peak shows two maxima at 239 and 310 nm, while those of the two (identical) spectra of the last eluting peaks are found at 230 and 320 nm.

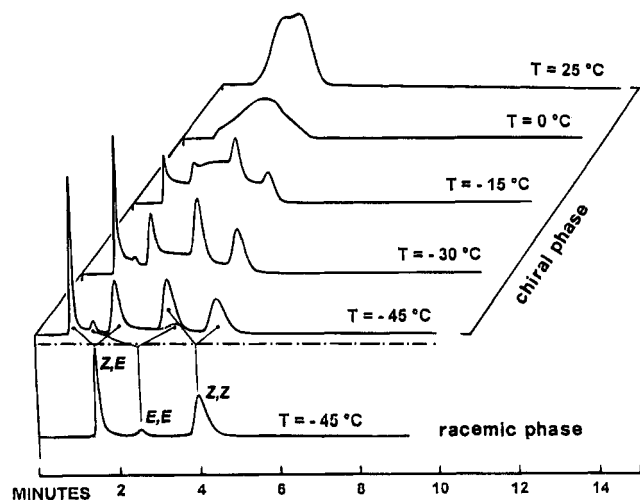


Figure 3. UV detected (320 nm) dynamic HPLC of **1b** on the (*R,R*)-CSP and on the racemic stationary phase (see Table 2 for other details).

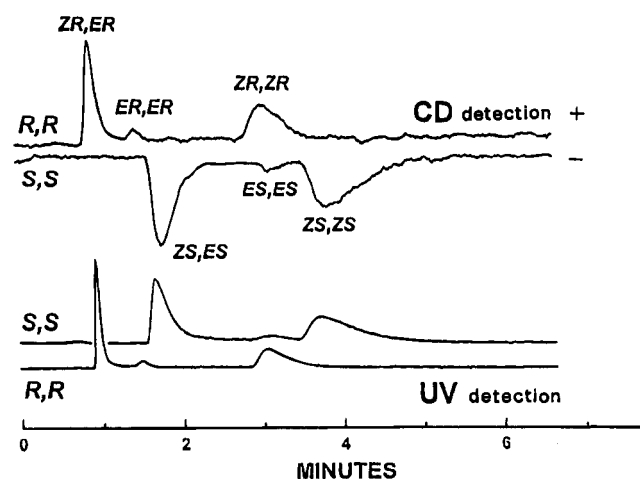


Figure 4. UV (320 nm) and CD (320 nm) detected by low-temperature ($-45\text{ }^{\circ}\text{C}$) HPLC of (*R,R*)-**1b** and (*S,S*)-**1b** on the (*R,R*)-CSP (see Table 2 for other details).

The difference in the population of the *Z,E* atropisomers between **1a** and **1b** can be in part explained considering a statistical factor favoring the *Z,E* atropisomer of the latter, as it can exist in the two equivalent *1E,5Z* and *1Z,5E* conformations.

When the *R,R* enantiomer of **1b**, resolved at room temperature by preparative chiral HPLC, is passed through the analytical column at $-45\text{ }^{\circ}\text{C}$ and monitored by simultaneous UV and CD detections at 320 nm, the three peaks show positive CD signals while negative CD signals are observed in the case of the *S,S* enantiomer (Figure 4). From the separate chromatography of the two enantiomers it is clearly seen that peak overlapping occurs for the third eluted atropisomer of *R,R* configuration and the second eluted one of *S,S* configuration; thus, the complete elution order of **1b** from (*R,R*)-CSP at $-45\text{ }^{\circ}\text{C}$ is *ZR,ER*; *ER,ER*; *ZS,ES*; *ZR,ZR*; *ES,ES*; and *ZS,ZS* in order of increasing capacity factor.

As previously mentioned we were able to assign, by X-ray diffraction, the absolute *R,R* configuration (Figure

(8) Peak areas were determined by digital integration of the UV signal at 320 nm for **1b** and at 310 nm for **1a**. In these cases in principle the relative intensities might not correspond exactly to the actual distribution of the atropisomers, owing to their diastereomeric relationship.

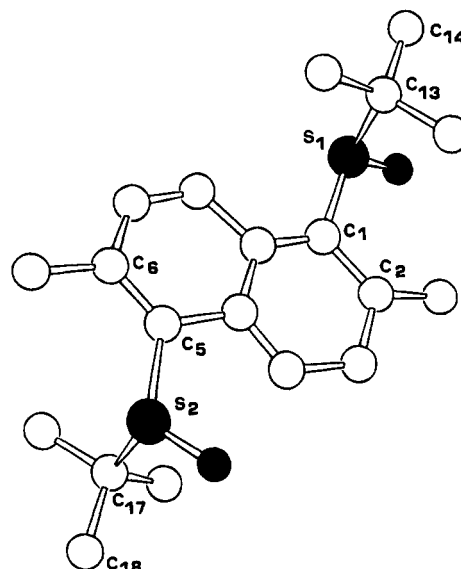


Figure 5. View of the X-ray diffraction structure of the first eluted enantiomer of **1b** [(*ZR,ER*)-**1b**] (atropisomer IX in Chart 2) showing the *R,R* absolute configuration at the sulfur atoms (the S=O moieties are displayed in black).

5) at the sulfur atoms of the first eluted enantiomer of **1b** (*ZE* atropisomer IX in Chart 2).⁹

It has been therefore demonstrated that all the predicted 10 stereoisomers of **1** can be separated and their configuration and conformation unambiguously assigned by the combined use of NMR and chiral HPLC techniques at variable temperature, as well as by the use of single-crystal X-ray analysis of a single enantiomer of **1b** obtained by preparative chiral chromatography.

Experimental Section

Materials. **2,6-Dimethyl-1,5-bis(2-methyl-2-propylsulfynyl)naphthalene (1).** To a cooled ($-30\text{ }^{\circ}\text{C}$) solution of the corresponding disulfide (910 mg, 2.75 mmol in 30 mL of chloroform) was added 950 mg (5.50 mmol) of 3-chloroperbenzoic acid in small portions. After being stirred for 1 h at $-30\text{ }^{\circ}\text{C}$ the mixture was washed with saturated NaHCO_3 , dried over sodium sulfate, and concentrated to give 850 mg of the title compound. Preparative HPLC on an axially compressed column (LiChroprep Si60, 15–25 μm , $35 \times 4\text{ cm}$, eluent $\text{CH}_2\text{Cl}_2/\text{EtOAc}$ 80:20) gave 560 mg of **1a** (first eluted) and 210 mg of **1b**. **1a.** IR (KBr): ν 1043. Anal. Calcd for $\text{C}_{20}\text{H}_{28}\text{O}_2\text{S}_2$: C, 65.89; H, 7.74; S, 17.56. Found: C, 65.81; H, 7.70; S, 17.60. **1b.** IR (KBr): ν 1048. Anal. Calcd for $\text{C}_{20}\text{H}_{28}\text{O}_2\text{S}_2$: C, 65.89; H, 7.74; S, 17.56. Found: C, 65.85; H, 7.75; S, 17.60.

2,6-Dimethyl-1,5-bis(2-methyl-2-propylthio)naphthalene. To a solution of 1,5-dibromo-2,6-dimethylnaphthalene (3.14 g, 10 mmol in 40 mL of *n*-butanol) were added sodium 2-methyl-2-propanethiolate (2.24 g, 20 mmol) and palladium tetrakis(triphenylphosphine) (0.24 g, 0.2 mmol) under argon atmosphere. The solution was refluxed for 6 h, and after the solvent was removed at reduced pressure, the residue was taken up with hexane and filtered through a short pad of silica. After removal of the solvent, crystallization of the solid residue from chloroform/hexane gave 1.50 g of the title compound. ^1H NMR (CDCl_3 , 300 MHz) δ : 1.26 (18H, s, $(\text{CH}_3)_3\text{C}$), 2.77 (6H,

(9) The dihedral angle $\text{C}_2\text{--C}_1\text{--S}_1\text{--C}_{13}$ and $\text{C}_6\text{--C}_5\text{--S}_2\text{--C}_{17}$ are -96° and 97° , respectively, and the two *tert*-butyl groups adopt the same conformation around the S–C bonds, with dihedral angles of 179° ($\text{C}_1\text{--S}_1\text{--C}_{13}\text{--C}_{14}$) and -173° ($\text{C}_5\text{--S}_2\text{--C}_{17}\text{--C}_{18}$). It is worthwhile mentioning that the MM computed⁶ dihedral angles match these experimental values. The carbon atoms of the naphthalene ring lie essentially on a plane, while the *ortho* methyl groups are slightly twisted out of the naphthalene plane ($8\text{--}10^\circ$) pointing in the opposite direction of the nearest *tert*-butyl group.

s, CH₃Ar), 7.46 (2H, d, $J = 8.70$ Hz, H, Ar), 8.82 (2H, d, $J = 8.70$ Hz, H, Ar). ¹³C NMR (CDCl₃) δ : 23.19 (CH₃Ar), 31.72 ((CH₃)₃C), 49.62 ((CH₃)₃C), 128.70 (CH, Ar), 128.98 (C, Ar), 129.21 (CH, Ar), 136.90 (C, Ar), 142.72 (C, Ar). Anal. Calcd for C₂₀H₂₈S₂: C, 72.23; H, 8.49; S, 19.28. Found: C, 72.26; H, 8.40; S, 19.31.

NMR Spectroscopy. The variable-temperature spectra were recorded at 200, 300, and 600 MHz and the calibration carried out by means of the shift dependence of methanol (low temperatures) or ethylene glycol (high temperatures). The spectral simulations were performed with a two sites computer program¹⁰ based on the Bloch equations, and the best fit was judged by superimposing the plotted traces with the experimental spectra. The LIS experiments were obtained by adding increasing amounts of Eu(fod)₃ to CDCl₃ solutions of **1a**. The linear dependence of the displaced shifts *vs* the molar ratios had correlation coefficients equal to or better than 0.9987. The samples for the solid state ¹³C CP-MAS spectra (75.5 MHz) were fitted in ZrO₂ rotors spun at 3.8 KHz and the spectra acquired (about 2000 scans) with a standard cross polarization sequence using a contact time of 5 ms and a recycling time of 3 s.

Single-Crystal X-ray Structure of (Z,R,E)-1b** (Atropisomer IX in Chart 2).** Colorless prismatic crystals of **1a** and of the first eluted enantiomer of **1b** were obtained by slow evaporation from dichloromethane/hexane solutions. The crystal system of **1a** is orthorhombic, space group *Pca*2₁, with $a = 14.684(4)$ Å, $b = 6.265(3)$ Å, $c = 20.423(4)$ Å, $V = 1879(1)$ Å³, $Z = 4$, $M = 370.6$, $D_c = 1.31$ g cm⁻³, $\mu(\text{Cu K}\alpha) = 25.47$ cm⁻¹, $F(000) = 808.0$. Because of the poor quality of the crystals and the disorder around the sulfur atoms, the full-matrix least-squares anisotropic refinement could not go further than a R value of 0.119. Consequently, the geometry of the molecule is not good and this structure will not be further discussed. Nevertheless, the meso form and the conformation around the C_{Ar}-S bond are in agreement with that expected for **1a**, corresponding to the *Z,Z* atropisomer (II of Chart 1). The crystal system of **1b** is triclinic, space group *P*1, with $a = 8.541(1)$ Å, $b = 8.973(1)$ Å, $c = 6.861(1)$ Å, $\alpha = 106.26(1)^\circ$, $\beta = 106.99(1)^\circ$, $\gamma = 71.10(1)^\circ$, $V = 465.7(1)$ Å³, $Z = 1$, $M = 370.6$, $D_c = 1.32$ g cm⁻³, $\mu(\text{Cu K}\alpha) = 25.69$ cm⁻¹, $F(000) = 202.0$. All measurements were made on a Rigaku AFC5R diffractometer with graphite monochromated Cu K α radiation and a 12 KW rotating anode generator. Cell constants and an orientation matrix were obtained from a least-squares refinement using the setting angles of 25 carefully centered reflections in the range $40^\circ < 2\theta < 80^\circ$. The data were

collected at room temperature using the $\theta - 2\theta$ scan technique to a maximum 2θ value of 124° . The ratio peak counting time to background counting time was 2:1. Of 1534 independent reflections collected for compound **1b**, 1241 had $F_o > 6.0\sigma(F_o)$. The intensities of three representative reflections, which were measured after every 150, remained essentially constant throughout data collection indicating crystal and electronic stability (no decay correction was applied). An empirical absorption correction based on azimuthal scans of several reflections was applied to intensities. The data were corrected for Lorentz and polarization effects. The structures were solved by direct methods with the SIR92 program.¹¹ The non-hydrogen atoms were refined anisotropically. Their positions and thermal parameters were refined assuming the riding model approximation. Isotropic and anisotropic refinement was carried out by the full-matrix least-squares method minimizing the function $\sum w(|F_o| - |F_c|)^2$, where $w = (a + |F_o| + c|F_o|^2)^{-1}$ with a and c equal to $2F_{o(\min)}$ and $2F_{o(\max)}$, respectively, and converged to $R = 0.081$ and $R_w = 0.111$. As the space group is polar, the refinement was also performed on the enantiomeric structure which converged to $R = 0.083$ and $R_w = 0.114$. When the R -factor ratio test is applied,¹² an R value of 1.022 is obtained, which is greater than the value $R_{1,1252,0.005} = 1.003$ obtained by interpolation from the Hamilton tables at the 0.005 significance level for a one-dimensional hypothesis and 1252 degrees of freedom. Hence, the probability of the inverted model (i.e., *SS*) being correct can be rejected at the 99.5% confidence level. A listing of fractional atomic coordinates, thermal parameters, relevant atomic distances and angles for **1b** have been deposited at the Cambridge Crystallographic Data Centre. The coordinates can be obtained, on request, from the Director, Cambridge Crystallographic Data Centre, 12 Union Road, Cambridge, CB2 1EZ, UK.

Chromatographic Measurements. The HPLC apparatus, cooling devices for low-temperature chromatography, and on-line CD detection have been described.¹³

Acknowledgment. Thanks are due to the Highfield NMR Laboratory of the University of Florence and to Mr. M. Lucchi for the 600 MHz spectra. This work was carried out with the financial support of the National Research Council (CNR) and Ministry of the University of Scientific Research (MURST), Rome.

(11) SIR92: Altomare, A.; Cascarano, G.; Giacobozzo, C.; Guagliardi, A.; Burla, M. C.; Polidori, G.; Camalli, M. *J. Appl. Crystallogr.* **1994**, *27*, 435.

(12) Hamilton, W. C. *Acta Crystallogr.* **1965**, *18*, 502.

(13) Casarini, D.; Lunazzi, L.; Pasquali, F.; Gasparrini, F.; Villani, C. *J. Am. Chem. Soc.* **1992**, *114*, 6521.

(10) Bonini, B. F.; Grossi, L.; Lunazzi, L.; Macciantelli, D. *J. Org. Chem.* **1986**, *51*, 517.